

## A global measure for depth of investigation

Anders Vest Christiansen<sup>1</sup> and Esben Auken<sup>2</sup>

### ABSTRACT

We tested a new robust concept for the calculation of depth of investigation (DOI) that is valid for any 1D electromagnetic (EM) geophysical model. A good estimate of DOI is crucial when building geologic and hydrological models from EM data sets because the validity of the models varies strongly with data noise and the resistivity of the layers themselves. For diffusive methods, such as ground-based and airborne electromagnetic, it is not possible to define an unambiguous depth below which there is no information on the resistivity structure and a measure of DOI is therefore to what depth the model can be considered reliable. The method we presented is based on the actual model output from the inversion process and we used the actual system response, contrary to assuming, e.g., planar waves over a homogeneous half-space, the widely used skin depth calculation. Equally important, the data noise and the number of data points are integrated into the calculation. Our methodology is based on a recalculated sensitivity (Jacobian) matrix of the final model and thus it can be used on any model type for which a sensitivity matrix can be calculated. Unlike other sensitivity matrix methods, we defined a global and absolute threshold value contrary to defining a relative (such as 5%), sensitivity limit. The threshold value will apply to all 1D inverted data and will thus produce comparable numbers of DOI.

### INTRODUCTION

For diffusive methods, like ground-based or airborne EM, there is no specific depth below which there is no information on the resistivity structure of the ground, so it is of great interest to ascertain to what depth the model can be considered reliable. This means that

any method for calculating the depth of investigation (DOI), at some point, needs to assign a number representing a required level of information. In most cases, this number is relative stating, for instance, 5% of the total sensitivity.

We present a new, robust, and simple concept for the calculation of DOI that is valid for any 1D EM and DC geophysical model using a global and absolute threshold value.

Several concepts for the calculation of DOI or penetration depth have been presented over the years. For EM methods, the simplest form is based on the diffusion depth of a planar wave in a full-space, here in the time-domain at the time  $t$ , on a full-space with conductivity  $\sigma$  (Ward and Hohmann, 1988):

$$z_d = \sqrt{\frac{2t}{\mu\sigma}} \quad (1)$$

The time  $t$  that enters the equation is typically the last time-gate of the measurement. A similarly simple expression can be written for frequency-domain methods. Although simple, this approach is problematic. Just think about the extreme case of having only a single very late and noisy gate-value left out of a full decay.

Another group of methods is based on empirical formulas or tables based on model studies or thin sheet calculations (Banerjee and Pal, 1986; Huang, 2005; Szalai et al., 2009).

These methods are fast and simple, but they suffer from one or more of the following problems:

- 1) The system transfer function or system geometry is not considered.
- 2) The actual model in question is not considered (e.g., a half-space is assumed). The DOI will depend strongly on the actual model.
- 3) Noise on the data is not considered. More noise obviously decreases the DOI.
- 4) The actual number of data points is not considered — e.g., using diffusion depth based on the lowest frequency/latest time.

Manuscript received by the Editor 9 October 2011; revised manuscript received 8 February 2012; published online 10 July 2012.

<sup>1</sup>Geological Survey of Denmark and Greenland (GEUS), Højebjerg, Denmark and Aarhus University, Institute for Geoscience, HydroGeophysics Group, Department of Geoscience, Aarhus, Denmark. E-mail: avc@geus.dk.

<sup>2</sup>Aarhus University, Institute for Geoscience, HydroGeophysics Group, Department of Geoscience, Aarhus, Denmark. E-mail: esben.auken@geo.au.dk.

© 2012 Society of Exploration Geophysicists. All rights reserved.

- 5) The DOI is based on a relative number, such as 5% of the total sensitivity. This approach has the unfortunate effect that adding data points can decrease the DOI. This is the case if early time data are added to a TEM sounding; the relative weight moves closer to the surface and the DOI decreases.

Oldenburg and Li (1999) propose a method for DC that involved separate inversions with different objective functions. The difference between the models then is used to determine if the model is data-driven or driven by the regularization of the inversion. This methodology since has been successfully used for many different applications including airborne EM (Lane et al., 2004) and ground conductivity meters (Brosten et al., 2011). The approach ensures that the full system transfer function is used, including the actual data set, on the model in question. However, two issues remain with the method. First, the full inversion needs to be carried out at least twice, or ideally three times, which is not feasible for full scale airborne data sets. Secondly, the resulting DOI value will be affected by the total regularization. For example, setting a tighter constraint to the reference model will give the impression of a smaller DOI, whereas stronger vertical constraints, i.e., large vertical smoothness, will have the opposite effect.

DOI also can be estimated by defining relative differences between forward responses for variations of the model investigated. Szalai et al. (2011) uses this approach to define what is called a “detectability level.” Different variations of the measure are widely used for survey design studies. Probably, the most extensive inves-

tigation related to the DOI is performed using an approach of the Monte Carlo family. Minsley (2011) uses a Markov-chain Monte-Carlo (MCMC) approach to undertake an exhaustive model space search for the most probable model fitting a given data set, taking the full system transfer function, data noise, etc. into account. Having searched the model space exhaustively, equivalence problems and other model-space related issues can be included in the DOI investigations, which is normally not possible. It is still necessary, though, to set a threshold value for the DOI if a single number for DOI is required. The obvious drawback of this approach is the massive computational cost, which limits it to selected soundings in large-scale surveys.

The method proposed here is based on a recalculated Jacobian matrix of the final 1D model. It is similar to the approach by Oldenburg and Li (1999) in the sense that it uses the full system transfer function and system geometry, all the data, and the noise on the data. However, in this approach, it is not necessary to perform additional inversions; only one extra forward response is required in some cases. Also, we will show that the DOI is defined globally for any DC or EM data set with an absolute threshold value for the minimum amount of information required for something to be “resolved.” Contrary to the approach by Oldenburg and Li (1999), the constraints do not play a direct role and the DOI value obtained is a measure of the capability of the measured data and their uncertainty to resolve the given model. The model itself is of course a result of data, data uncertainty, inversion method, and regularization.

## METHODOLOGY

The methodology for calculating the DOI is based on a recalculated Jacobian matrix from a 1D model. The methodology as presented here is applicable to 1D models but can be extended to 2D and 3D models as well. Working with global and absolute threshold values requires a relative, data-type, independent relation between the model space and data space, which we obtain by working in the logarithmic model and data spaces. In the case that this is not possible, the global threshold value is not applicable and threshold values for system and survey specific setups must be established. For a given model, the DOI calculations solely include information from the part of the Jacobian relating to the observed data. This means that lateral or vertical model constraints or a priori information, which also contributes information to the model, is not included.

The workflow includes the following steps:

- 1) Starting from a measured data set, we invert the data into a smooth or a few-layered model. The inversion includes the data uncertainty, estimated from the data stack, and the regularization method of the chosen inversion algorithm.
- 2) We then construct a subdiscretized version of the model from step 1 to be able to evaluate the DOI precisely for models with few layers. For multilayer models (smooth models), this step can be skipped because the model is already finely discretized.
- 3) We then calculate the Jacobian for the subdiscretized model.
- 4) The Jacobian is finally used to compute the cumulated sensitivities from which we can deduct the DOI.

We will begin with the Jacobian. The inverted model  $m$  is subdiscretized to create a new model called  $m^*$  for  $M$  layers  $m = (\log(\rho_1), \dots, \log(\rho_M), \log(t_1), \dots, \log(t_{M-1}))$ , where  $\rho_{1 \dots M}$  are the layer resistivities and  $t_{1 \dots M-1}$  are the layer thicknesses. The resistivities of the layers in  $m^*$  (represented by the dots in

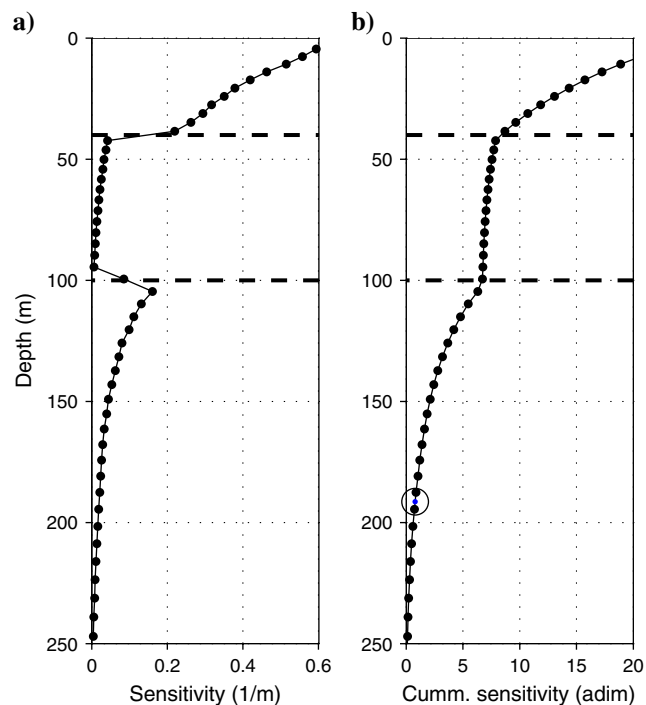


Figure 1. Sensivities calculated for a rediscretized version of the base model indicated by the black dashed lines. The layer resistivities are, starting from the top 40, 200, and 5 ohm-m. Thickness are 40 and 60 m. The left plot shows the entries of the  $s^*$ -vector of equation 3. The right plot shows the cumulated sensitivities  $S$  of equation 4, i.e., the total sensitivity in a given depth and downward. The circle indicates the DOI given by the global threshold value, the value is 0.8.

Figure 1) are repeated values of the resistivities of  $m$ . To comply better with the underlying physics, weighted averages are used across layer boundaries; for EM methods, the averages are calculated from the conductivities whereas for DC methods we use resistivities. For the model  $m^*$ , we then calculate a standard sensitivity (Jacobian) matrix,  $G$ , using

$$G_{ij} = \frac{\partial \log(d_i)}{\partial \log(m_j)}, \quad (2)$$

which represents the sensitivity to the  $i$ th data point  $d_i$  from the  $j$ th model parameter  $m_j$ . Taking the sum of each column of  $G$  and normalizing for the standard deviation of the data points,  $\Delta d_i$ , we get the error normalized sensitivity  $s$  of each of the model parameters  $j$  in  $m^*$  according to

$$s_j = \frac{\sum_{i=1}^N G_{ij}}{\Delta d_i} \quad (3)$$

where  $N$  is the number of observed data points in  $d$ . The vector  $s$  now holds the total error normalized sensitivities for the model parameters with respect to all the data.

For general purposes and plotting, it is handy to state the error and thickness normalized sensitivity  $s^*$  to remove the effect of varying thickness of the layers:

$$s_j^* = \frac{\sum_{i=1}^N G_{ij}}{t_j \Delta d_i}, \quad (4)$$

where  $t_j$  is the thickness of the  $j$ th layer in the subdiscretized model  $m^*$ . Note that  $s^*$  is not defined for the last semi-infinite layer.

As an example, we take a SkyTEM system (Sørensen and Auken, 2004) with the last gate at 3 ms. Assuming a simple three-layer model, we can plot the entries of  $s^*$  versus depth as shown in Figure 1a. As expected, the sensitivity to the resistive second layer is low, whereas there are high sensitivities to layers one and three, which are more conductive.

Summing the layer sensitivities of equation 2 upward, we get the cumulated sensitivities  $S$ :

$$S_j = \sum_{i=M,-1}^j s_i, \quad (5)$$

where  $M$  is the number of layers in  $m^*$ . The entries of  $S$  are shown in Figure 1b. This plot expresses the total sensitivity for a given depth and downward.

Finally, we set a threshold value that indicates the minimum amount of sensitivity needed for indicative information. In the example in Figure 1, we settled on 0.8 as the threshold value, giving a DOI of approximately 190 m.

Setting the threshold value is very much a question of fine-tuning based on experience, intuition, and comparing different models with different methods. The threshold value suggested here is purely empiric, but it has been tested on many different models and with different systems covering ground conductivity meters to the largest airborne TEM systems, and it produces results that are in agreement with one's intuition and other measures of DOI for the given method. Setting a higher threshold value will decrease the DOI,

and a lower value will increase the DOI. In the experimental fine-tuning we have considered values in the range from 0.6 to 1.2. For the example in Figure 1, these values produce DOI values between 175 m and 202 m, compared to the selected value of 190 m. The same threshold value (0.8) is used for all examples in this paper.

## SYNTHETIC EXAMPLES

### Homogeneous half-space, different data types

The first example shows the DOI methodology described above applied to different data types over the same homogeneous half-space. The data types that we will compare are:

- DC resistivity data in a Schlumberger sounding mode with AB/2 values ranging from 1.0 to 200 m, distributed with 10 points per decade to a total of 24 data points
- Ground conductivity meter (GCM) data with the Tx-Rx at 95 cm and at 10,000 Hz. Three dipole separations of 0.98, 1.89, and 3.77 m measured with vertical and horizontal dipoles to a total of six data points
- Helicopter-borne frequency domain (HEM) data from the Resolve system with five vertical and one horizontal magnetic dipole at five frequencies of 390, 1798, 3242 (horizontal), 8177, 39,470, and 132,700 Hz. Dipole separations of 7.9 m for the vertical dipoles and 9 m for the horizontal set. Flying altitude 30 m.
- Helicopter-borne time-domain data from the SkyTEM system, with two transmitter moments covering the time range from 17 to 2.81 ms (later gates are assumed to be noisy) with a total of 30 time gates. Square waveform with a turn-off time of 4.5  $\mu$ s transmitted in a hexagonal transmitter loop, with the receiver essentially in a central-loop position. Flying altitude 30 m.

Obviously, the data noise plays an important role in the DOI calculations in these cases, but to simplify things, we will assume 5% noise on all data points for all data types.

The DOI computations are shown as absolute sensitivities (Figure 2a) and as cumulated sensitivities (Figure 2b). Note that both axes are logarithmic to cover the larger range when dealing with methods that have very different sensitivities and target depths.

Unsurprisingly, the DC and GCM methods have the highest sensitivities at the top, whereas the SkyTEM-type system has the deepest information. The DOI values fall more or less in the expected range except maybe the DC Schlumberger, which reaches beyond 100 m. Keep in mind though that the traditional *focus depth* of DC methods refers to 50% total sensitivity, and from Figure 2 it is obvious that the DC sensitivity has a very long tail in the deepest parts.

### Layered half-space, different data types

The second example shows the behavior of different systems over a layered earth. To cover depth ranges including GCM methods and airborne TEM, the depth to layer boundaries are increasing logarithmically as shown in Figure 3a. Furthermore, the layer boundaries are indicated with thin lines in Figure 3b and 3c. Having a layered half-space, it becomes evident that the EM methods are sensitive primarily to the high-conductivity layers (for example layer three), while the DC method mainly loses sensitivity at the boundaries, which decreases its total DOI from more than 110 m in the homogeneous half-space to 42 m for this layered half-space. The

Resolve-type system also sees a decreasing DOI from more than 50 m to just under 20 m. This is, in this case, due to the conductive third layer shielding the signal from going deeper. The GCM-type system also loses its power in the third layer, with a DOI of 8.5 m,

whereas the SkyTEM system benefits from the deep good conductor maintaining a DOI of close to 200 m.

**Synthetic valley model, TEM data**

This example shows the behavior of the DOI calculation when applied to data simulating real field data from a buried valley

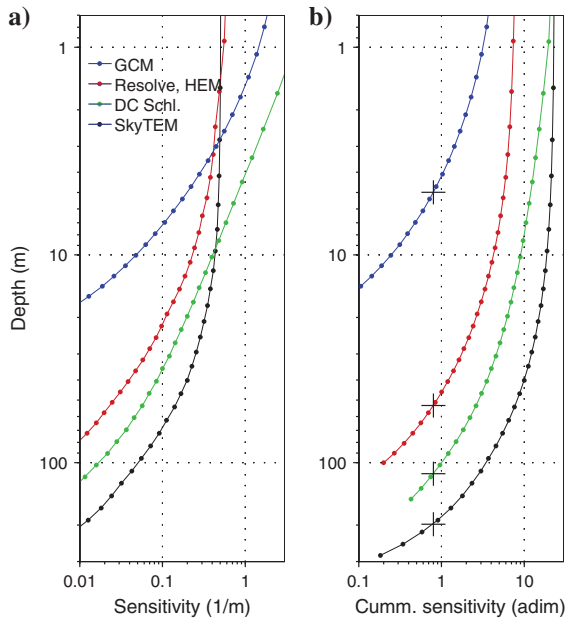


Figure 2. Sensitivities and DOI for different data types: (a) shows the sensitivities,  $s^*$  of equation 4, (b) shows the cumulated sensitivities  $S$  of equation 5. The blue line refers to ground GCM data, the red line to Resolve HEM data, the green line to DC Schlumberger data, and the black line to SkyTEM data. The plus indicates where the cumulated sensitivities intersect the global threshold value of 0.8. DOI values from top to bottom are 5.0 m for GCM, 53.1 m for Resolve HEM, 113.2 m for DC Schlumberger, and 198.0 m for SkyTEM. Note that to get all systems represented in the same plot the axes are logarithmic.

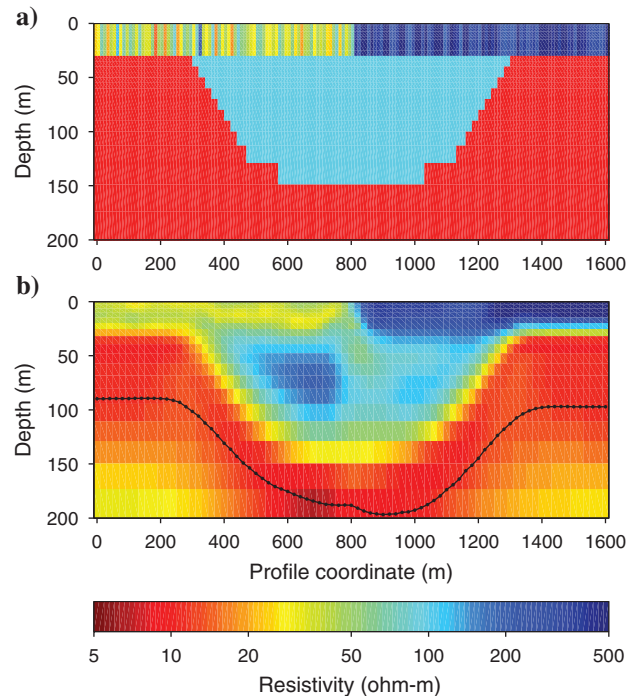
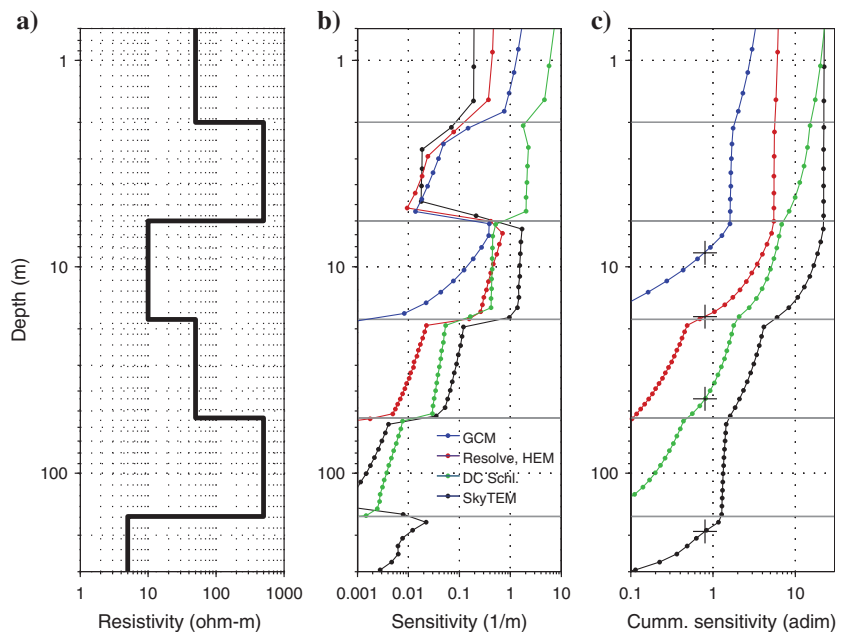


Figure 4. Synthetic example over a buried valley model using ground-based TEM data. The synthetic model is shown in (a), whereas (b) shows the inverted result together with the DOI-information.

Figure 3. Sensitivities and DOI for different data types on a layered half-space: (a) shows the sensitivities  $s^*$  of equation 4, (b) shows the cumulated sensitivities  $S$  of equation 5. The blue line refers to ground GCM data, the red line to HEM data, the green line to DC Schlumberger data, and the black line to SkyTEM data. The plus indicates where the cumulated sensitivities intersect the global threshold value of 0.8. DOI values from top to bottom are 8.6, 17.8, 42.3, and 193.4 m. Layer boundaries in the underlying model are indicated by the gray lines.



structure (Jørgensen et al., 2003; Auken et al., 2008). The model is a full 3D model with a near-surface inhomogeneous layer on top of a 2D valley structure. We are simulating a ground-based TEM instrument in a central-loop configuration with a  $40 \times 40 \text{ m}^2$  loop. The data have been perturbed with a real noise model and then processed and inverted as if they were field data (Auken et al., 2009). The inversion is carried out using the laterally constrained inversion (LCI) methodology as described in Auken et al. (2005). The general resolution results over these synthetic models are discussed in detail in Auken et al. (2008) and Jørgensen et al. (2003).

As expected, the DOI is strongly affected by the geology, going deep in the central parts of the valley, while being shallower on the flanks where the signal enters the low-resistivity layer quickly. Likewise, the overburden has the anticipated effect — although weak — acting as a shield when it is more conductive (to the left in Figure 4) preventing a DOI as deep as where the overburden is more resistive (to the right in Figure 4). Below the DOI, the model slowly returns to the starting model, showing that only very limited model information is present in the data. Keep in mind, though, that the rate of returning to the starting model is heavily dependent on the strength of the vertical constraints in the inversion model.

**FIELD EXAMPLES**

**Multielectrode DC and ground-based TEM data**

To demonstrate the performance of the DOI approach presented in this paper, we will first show an example from a field study on a buried valley structure in Denmark that was measured using ground-based TEM and multielectrode DC data (Figure 5). The data and inversion strategy are presented in detail in Christiansen et al. (2007). The full DC data set is concatenated from two profiles on either side of a road at coordinate 465 m. The electrode separation is 5 m, measured using a gradient array protocol (Dahlin and Zhou, 2006) with the longest configurations having 360 m between current electrodes. The model section from the LCI inversion of the DC data alone in Figure 5a clearly shows the effect of the missing data from the deeper part of the section in the DOI calculations with the tapering at the ends of the two original profiles. The maximum DOI is close to 100 m.

The LCI profile of the ground-based TEM data is shown in Figure 5b. The TEM data are collected using a combined central-loop and offset-loop configuration for large penetration depth without sacrificing the shallow information. The latest time gate is 7 ms. The figure reveals a much deeper DOI that clearly finds the bottom of the buried valley, but the surface near model details are simplified compared to the DC result. The DOI of the TEM data goes deeper than 200 m. Finally, Figure 5c shows

the mutually and laterally constrained inversion result combining the information from the DC data and the TEM data in the same inversion. The DOI line now clearly identifies the TEM soundings where the DOI goes deep. The model result is basically the DC result in the shallow parts and the TEM result in the deep parts with the joint efforts getting the thick resistive layer right at the resistivity and the thickness.

In this case, the data have been inverted using lateral constraints to migrate information between soundings of the same data type and mutual constraints between the DC data to the TEM data. The result is a visibly improved resolution of the subsurface. The DOI assist the interpreter to quickly evaluate the results and estimate their validity.

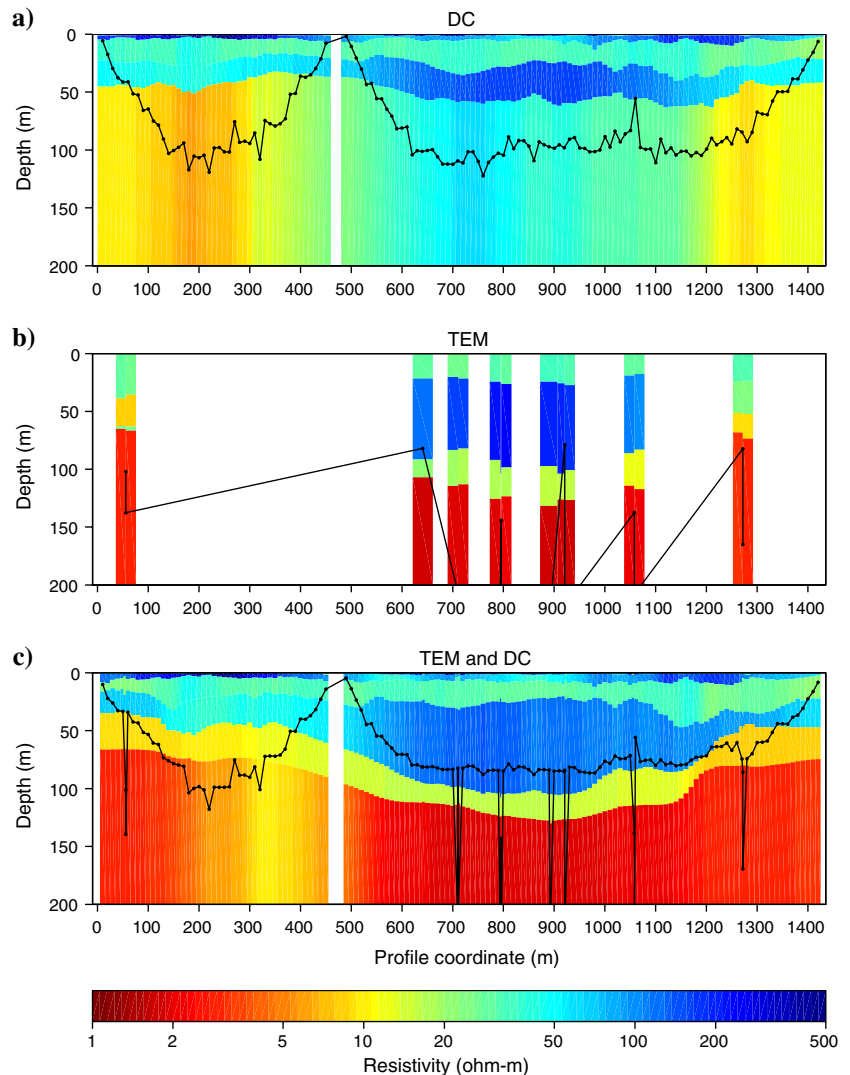


Figure 5. Field example with DC and ground-based TEM data over a buried valley. The inverted multielectrode DC model is shown in (a), whereas (b) shows the inverted result of the TEM data alone, and (c) shows the result of a mutually and laterally constrained inversion of both data sets (Christiansen et al., 2007). All panels show the DOI with the dotted line in black. The abrupt changes in the DOI at the locations of the TEM soundings in (c) clearly visualize the much higher DOI for TEM compared to DC.

## Large-scale SkyTEM survey, Denmark/Germany border region

The last field example is from a SkyTEM survey from the border region between Denmark and Germany and shows the use of the DOI information when dealing with large-scale surveys. The total survey area is 680 km<sup>2</sup> with a total of 3330 line kilometers flown. Figure 6a shows the north–south profile indicated by the black line in Figure 6b. The profile crosses a known graben structure in the area, and the north flank is clearly visible around profile coordinate 5000 m. It is clear that the DOI is strongly affected by the geologic variations along the profile, primarily determined by the depth and thickness of the conductive layer.

In large-scale surveys, the products on which the interpretation is based often comprises area covering maps of interval resistivities. For deep map slices, it is important to include the DOI information to avoid interpretation of features that are not an effect of the data

information. This can be facilitated through color-fading as suggested by Oldenburg and Li (1999) or a degree of blanking of areas below the DOI. Figure 6b shows an interval resistivity map from the elevation interval (–150; –160 m), where areas below the DOI have been blanked with the gray shading. It immediately becomes clear that large areas in this depth are well below the DOI and they should therefore be treated with care or omitted in the geologic interpretation process.

## DISCUSSION

### DOI accuracy

The subdiscretization of the inverted model obviously has an effect on the DOI results. If one has too few layers, the DOI calculations will be inaccurate due to interpolation errors and having many layers will increase the computation time. In the synthetic examples shown in Figure 1 to Figure 3, the model was subdiscretized into many layers to assist the visual understanding of the concept. In reality, it is not necessary to subdiscretize a model with few layers into more than around 12–15 layers to obtain a reasonable precise DOI, e.g., within roughly 3–5 meters for calculations down to 250 m.

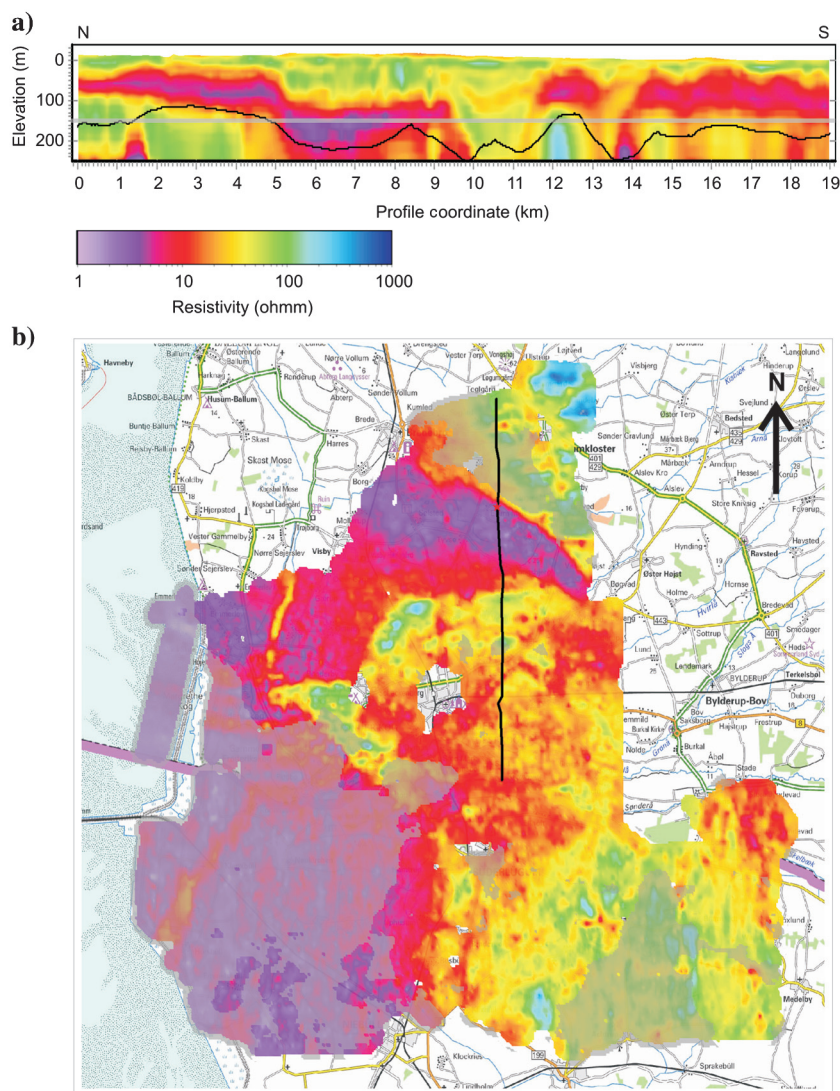


Figure 6. Field example with SkyTEM data: (a) shows a section through the northern part indicated by the black line in (b). The DOI is shown in black. (b) Shows an interval resistivity map for the elevation slice –150 to –160 m. Areas below the DOI are blanked by the semitransparent gray shading. The map area is approximately 40 by 40 km.

### A single-value DOI for diffusive models?

We have here consistently shown the DOI as a single number, even though this is somewhat contradicting to the diffusive nature of EM and DC methods, suggesting that information gradually fades away with depth. As discussed briefly in context with the field example, this gradual transition can be facilitated through color fading as suggested by Oldenburg and Li (1999) or a degree of blanking of areas below the DOI, although a color-fading still requires someone to settle on the amount of fading for a given sensitivity content. Also, end-users of geophysical models are rarely geophysicists themselves and request easy-to-interpret maps and sections. Our experience is that the DOI, as presented here, get the crucial information across with a minimum amount of information load. We have tried to present DOI with an upper and a lower value as well, but that has not been well received. Geophysicists wanting to take full advantage of the DOI computations could easily use the full sensitivity kernels of equations 2–4 for full access to fading, etc.

### Equivalent models

The method proposed here does not take into account equivalent models that might fit the observed data equally well. In other words, we assume that the model at hand is the best model and the DOI relates only to this model and the sensitivities calculated for this model. This

means that we cannot answer questions such as “is it possible that a conductive layer is present 10 m below the DOI?”

This issue can only be addressed in full by the use of exhaustive methods like the MCMC discussed earlier (Minsley, 2011). The method described by Oldenburg and Li (1999) where three individual inversions with varying reference models are used will address the issue of equivalency to some degree because the alternative inversions suggest how much the model can be pulled in a given direction without violating the data. If, for instance, we consider EM data from a generally conductive half-space with a resistor at depth, the DOI calculations suggested here will put the DOI close to the boundary between the conductor and resistor at depth because the sensitivity drops rapidly at that border. The method by Oldenburg and Li (1999) will most likely put it deeper because the different inversions will reveal a minimum thickness of the resistor.

Another aspect relating to this is connected to data sets that cannot be fitted within the assigned data standard deviations. In this case, the DOI values obtained will be too deep because assigning a higher standard deviation that will allow you to fit the data will inevitably decrease the DOI. In other words, it is essential for the validity of the DOI computations on a given model that the observed data are fitted within the assigned standard deviations and that these standard deviations are estimated correctly for the data.

### Constraints versus data

Consider a model section where the data have been inverted using lateral constraints as well as a priori knowledge added from boreholes. In that case, it can often be difficult to judge which parts of the model are data-driven and which parts are driven by the constraints and a priori information. If carefully added, the constraints often supply valuable input to the inversion by including information on geologic variability (Auken et al., 2005).

The DOI approach presented here is based only on part of the Jacobian referring to the observed data. Hence, plotting the DOI on top of a section will allow discrimination of the data-driven parts and the constraints and a priori driven parts of the model. This information can assist the interpreter to quickly evaluate the results and estimate the validity of the results.

### CONCLUSION

We have presented a new robust concept for the calculation of DOI that is valid for any 1D EM geophysical model.

The method is based on the actual model output from the inversion and includes the full system response and geometry, contrary to assuming, e.g., plane waves over a homogeneous half-space, the widely used skin-depth calculations. Equally important, the standard deviation on the data and the number of data points are integrated in our calculation.

The threshold limit will apply to all 1D inverted data and it is global in the sense that the same number can be used for airborne and ground based DC and EM methods.

A calculation of the DOI is crucial when building geologic or hydrological models from EM data as the validity of the models varies strongly with data noise and the resistivity of the layers themselves. Without the DOI estimate, it is next to impossible to judge when the information in the model is driven by the data or is just an effect of the starting model or the regularization of the inversion.

### ACKNOWLEDGMENTS

We want to thank GeoFysikSamarbejdet and the Danish Nature Agency, Ministry of the Environment, for supporting this work. We also thank Niels B. Christensen, Kurt Sørensen, and senior geophysicist Nikolaj Foged who have contributed greatly in numerous discussions. The transnational survey was made possible by the Leibniz-Institut für Angewandte Geophysik, Hannover, Germany (mapping with airborne geophysics, 2008/2009), the Danish Nature Agency and the Interreg IVB project CLIWAT (North Sea Region Programme 2007–2013 under the ERDF of the European Union). We also wish to thank Sándor Szalai, Colin Farquharson (editor), and two anonymous reviewers for their positive and constructive comments to the manuscript in the review process.

### REFERENCES

- Auken, E., A. V. Christiansen, B. H. Jacobsen, N. Foged, and K. I. Sørensen, 2005, Piecewise 1D laterally constrained inversion of resistivity data: *Geophysical Prospecting*, **53**, 497–506, doi: [10.1111/gpr.2005.53.issue-4](https://doi.org/10.1111/gpr.2005.53.issue-4).
- Auken, E., A. V. Christiansen, L. Jacobsen, and K. I. Sørensen, 2008, A resolution study of buried valleys using laterally constrained inversion of TEM data: *Journal of Applied Geophysics*, **65**, no. 1, 10–20, doi: [10.1016/j.jappgeo.2008.03.003](https://doi.org/10.1016/j.jappgeo.2008.03.003).
- Auken, E., A. V. Christiansen, J. A. Westergaard, C. Kirkegaard, N. Foged, and A. Viezzoli, 2009, An integrated processing scheme for high-resolution airborne electromagnetic surveys, the SkyTEM system: *Exploration Geophysics (USSR)*, **40**, no. 2, 184–192, doi: [10.1071/EG08128](https://doi.org/10.1071/EG08128).
- Banerjee, B., and B. P. Pal, 1986, A simple method for determination of depth of investigation characteristics in resistivity prospecting: *Exploration Geophysics (USSR)*, **17**, no. 2, 93–95, doi: [10.1071/EG986093](https://doi.org/10.1071/EG986093).
- Brosten, T. R., F. D. Day-Lewis, G. M. Schultz, G. P. Curtis, and J. W. Lane, 2011, Inversion of multi-frequency electromagnetic induction data for 3D characterization of hydraulic conductivity: *Journal of Applied Geophysics*, **73**, no. 4, 323–335, doi: [10.1016/j.jappgeo.2011.02.004](https://doi.org/10.1016/j.jappgeo.2011.02.004).
- Christiansen, A. V., E. Auken, N. Foged, and K. I. Sørensen, 2007, Mutually and laterally constrained inversion of CVES and TEM data — A case study: *Near Surface Geophysics*, **5**, 115–124, doi: [10.3997/1873-0604.2006023](https://doi.org/10.3997/1873-0604.2006023).
- Dahlin, T. L., and B. Zhou, 2006, Multiple-gradient array measurements for multi-channel 2D resistivity imaging: *Near Surface Geophysics*, **4**, 113–123, doi: [10.3997/1873-0604.2005037](https://doi.org/10.3997/1873-0604.2005037).
- Huang, H., 2005, Depth of investigation for small broadband electromagnetic sensors: *Geophysics*, **70**, no. 6, G135–G142, doi: [10.1190/1.2122412](https://doi.org/10.1190/1.2122412).
- Jørgensen, F., P. Sandersen, and E. Auken, 2003, Imaging buried Quaternary valleys using the transient electromagnetic method: *Journal of Applied Geophysics*, **53**, no. 4, 199–213, doi: [10.1016/j.jappgeo.2003.08.016](https://doi.org/10.1016/j.jappgeo.2003.08.016).
- Lane, R., R. Brodie, and A. Fitzpatrick, 2004, Constrained inversion of AEM data from the Lower Balonne area, southern Queensland, Australia. Lower Balonne Airborne Geophysical Project, CRC LEME OPEN FILE REPORT 163.
- Minsley, B. J., 2011, A trans-dimensional Bayesian Markov chain Monte Carlo algorithm for model assessment using frequency-domain electromagnetic data, *Geophysical Journal International*, **187**, no. 1, 252–272, doi: [10.1111/j.1365-246X.2011.05165.x](https://doi.org/10.1111/j.1365-246X.2011.05165.x).
- Oldenburg, D. W., and Y. Li, 1999, Estimating depth of investigation in DC resistivity and IP surveys: *Geophysics*, **64**, 403–416, doi: [10.1190/1.1444545](https://doi.org/10.1190/1.1444545).
- Sørensen, K. I., and E. Auken, 2004, SkyTEM — A new high-resolution helicopter transient electromagnetic system: *Exploration Geophysics*, **35**, no. 3, 191–199, doi: [10.1071/EG04194](https://doi.org/10.1071/EG04194).
- Szalai, S., A. Novak, and L. Szarka, 2009, Depth of investigation and vertical resolution of surface geoelectric arrays: *Journal of Environmental and Engineering Geophysics*, **14**, no. 1, 15–23, doi: [10.2113/JEEG14.1.15](https://doi.org/10.2113/JEEG14.1.15).
- Szalai, S., A. Novak, and L. Szarka, 2011, Which geoelectric array sees the deepest in a noisy environment? Depth of detectability values of multi-electrode systems for various two-dimensional models: *Physics and Chemistry of the Earth, Parts A/B/C*, **36**, 1398–1404, doi: [10.1016/j.pce.2011.01.008](https://doi.org/10.1016/j.pce.2011.01.008).
- Ward, S. H., and G. W. Hohmann, 1988, in M. N. Nabighian, ed., *Electromagnetic theory for geophysical applications in electromagnetic methods in applied geophysics*: SEG.